Sequential Measurements for Quantum-Enhanced Magnetometry in Spin Chain Probes

Victor Montenegro,[1,*] Gareth Siôn Jones,[2,†] Sougato Bose,[2,‡] and Abolfazl Bayat[1,§]
[1]Institute of Fundamental and Frontier Sciences, University of Electronic Science and Technology of China, Chengdu 610051, China
[2]Department of Physics and Astronomy, University College London, Gower Street, London WC1E 6BT, United Kingdom

(Received 2 February 2022; accepted 23 August 2022; published 13 September 2022)

Quantum sensors outperform their classical counterparts in their estimation precision, given the same amount of resources. So far, quantum-enhanced sensitivity has been achieved by exploiting the superposition principle. This enhancement has been obtained for particular forms of entangled states, adaptive measurement basis change, critical many-body systems, and steady state of periodically driven systems. Here, we introduce a different approach to obtain quantum-enhanced sensitivity in a many-body probe through utilizing the nature of quantum measurement and its subsequent wave function collapse without demanding prior entanglement. Our protocol consists of a sequence of local measurements, without reinitialization, performed regularly during the evolution of a many-body probe. As the number of sequences increases, the sensing precision is enhanced beyond the standard limit, reaching the Heisenberg bound asymptotically. The benefits of the protocol are multifold as it uses a product initial state and avoids complex initialization (e.g., prior entangled states or critical ground states) and allows for remote quantum sensing.

DOI: 10.1103/PhysRevLett.129.120503

Introduction.—Quantum sensing as a key application of quantum technologies [1,2] is now available in various physical setups, including photonic devices [3–8], nitrogen-vacancy centers [9–11], ion traps [12–16], superconducting qubits [17–20], cavity optomechanics [21–25], and cold atoms [26–31]. The precision for estimating an unknown parameter, quantified by the standard deviation σ, is bounded by the Cramér-Rao inequality $\sigma \geq 1/\sqrt{M\mathcal{F}}$, where M is the number of trials and $\mathcal{F}$ is the Fisher information [32,33]. For any resource T (e.g., time [34–37] or number of particles [38–40]), Fisher information, in general, scales as $\mathcal{F} \sim T^{\eta}$. While classical sensors at best result in $\eta = 1$ (standard limit), quantum sensors can achieve an enhanced sensitivity with $\eta = 2$ (Heisenberg limit) [38–40] or even $\eta > 2$ (super-Heisenberg limit) [41]. A fundamental open problem is to determine which quantum features can be exploited to achieve quantum-enhanced sensing.

Quantum mechanics is distinct from classical physics by two main features, namely, quantum superposition and quantum measurements. So far, the superposition principle has been exploited for achieving quantum-enhanced sensitivity through (i) exploiting the Greenberger-Horne-Zeilinger (GHZ) entangled states [38–40,42–46], (ii) the ground state of many-body systems at the phase transition point [8,47–57], (iii) the steady state of Floquet systems [58,59], (iv) adaptive [10,37,60–62] or continuous measurements [63–65], and (v) variational methods for optimizing the initial state as well as the measurement basis [66–68]. While these methods have their own advantages, they also suffer from several drawbacks. In GHZ-based quantum sensing, the preparation and manipulation are challenging [69–71], and interaction between particles deteriorates the sensitivity [52,72–74]. On the other hand, in both critical and Floquet many-body quantum sensors, the interaction between particles is essential and the system is more robust against imperfections. However, in such quantum sensors the region of quantum-enhanced sensitivity is very narrow [54,56]. Adaptive measurements are also not practically available in all physical platforms and training a programmable variational quantum sensor may take long times or face convergence issues [75]. Projective measurement, as another unique feature of quantum physics, has been employed for quenching many-body systems [76–80] which may induce new types of phase transitions [81–86]. One may wonder whether projective measurements and their subsequent wave function collapse can also be harnessed for obtaining quantum-enhanced sensitivity.

Here, we show that quantum measurement and its subsequent wave function collapse can indeed be used for achieving quantum-enhanced sensitivity. In our proposal, a many-body probe, initialized in a product state, is measured at regular times during its evolution without reinitialization. As the number of subsequent measurements increases, the protocol becomes far more efficient in using time as a resource, and the sensing precision is enhanced beyond the standard limit.

The model.—We consider a spin chain probe made of N interacting spin-1/2 particles for sensing a local magnetic field acting upon its first qubit via measuring the last one. For the sake of simplicity, we consider a Heisenberg Hamiltonian,

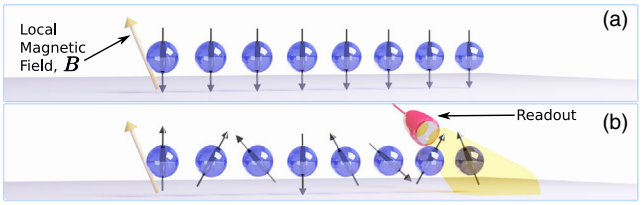

FIG. 1. Schematic of the protocol. (a) A spin chain probe is initialized in a product state for measuring a local magnetic field $\boldsymbol{B}$ at site 1. (b) The readout is performed sequentially on the last site, separated by intervals of free evolution.

$$H = -J\sum_{j=1}^{N-1}\boldsymbol{\sigma}_j\cdot\boldsymbol{\sigma}_{j+1} + B_x\sigma_1^x + B_z\sigma_1^z, \tag{1}$$

where $\boldsymbol{\sigma}_j = (\sigma_j^x, \sigma_j^y, \sigma_j^z)$ is a vector composed of Pauli matrices acting on qubit site j, J is the exchange interaction, and $\boldsymbol{B} = (B_x, 0, B_z)$ is the local magnetic field to be estimated. While we consider the unknown local field $\boldsymbol{B}$ to be in the xz plane, the generalization to the case of $B_y \neq 0$ is straightforward. The probe is initialized in the ferromagnetic state $|\psi(0)\rangle = |\downarrow\downarrow\downarrow\ldots\rangle$ as schematically shown in Fig. 1(a). Because of the presence of the local magnetic field $\boldsymbol{B}$, the system evolves under the action of H as $|\psi(t)\rangle = e^{-iHt}|\psi(0)\rangle$. During the evolution, the quantum state accumulates information about the local field $\boldsymbol{B}$, which can be inferred through later local measurements on the qubit site N, as shown in Fig. 1(b). As discussed in the Supplemental Material [87], the orientation of the Nth qubit follows the evolution of qubit 1 with a certain delay. This synchronization allows for remote sensing of $\boldsymbol{B}$ by looking at the dynamics at site N.

Sequential measurement protocol.—In a conventional sensing protocol, after each evolution followed by a measurement, the probe is reinitialized, and the procedure is repeated. Typically, initialization is very time consuming, making a significant overhead time for accomplishing the sensing. We propose a profoundly different yet straightforward strategy to use the time resources more efficiently by exploiting measurement-induced dynamics [76–80] and the distinct nature of many-body systems. After initialization, a sequence of n_{seq} successive measurements in a single basis is performed on the readout spin, each separated by intervals of free evolution, without reinitializing the probe. For simplicity, we first focus on the single-parameter estimation, namely, $B_z = 0$, in which B_x is the only parameter to be estimated. In this case, we assume that a simple fixed projective measurement in the σ_N^z basis is performed on the last qubit. The steps for the data gathering process is then as follows: (i) The system freely evolves according to $|\psi^{(i)}(\tau_i)\rangle = e^{-iH\tau_i}|\psi^{(i)}(0)\rangle$. (ii) The ith measurement outcome $|\gamma_i\rangle = |\uparrow\rangle, |\downarrow\rangle$ at site N appears with probability $p_{\gamma_i}^{(i)} = \langle\psi^{(i)}(\tau_i)|\Pi_N^{\gamma}|\psi^{(i)}(\tau_i)\rangle$, where $\Pi_N^{\uparrow} = (\mathbb{I} + \sigma_N^z)/2$ and $\Pi_N^{\downarrow} = (\mathbb{I} - \sigma_N^z)/2$ are spin projections. (iii) As a result of obtaining the outcome γ, the wave function collapses to the quantum state $|\psi^{(i+1)}(0)\rangle = [p_{\gamma_i}^{(i)}]^{-1/2}\Pi_N^{\gamma}|\psi^{(i)}(\tau_i)\rangle$. (iv) The new initial state from (iii) is substituted into (i), and the steps are repeated until n_{seq} measurements outcomes are consecutively obtained. Note that $|\psi^{(1)}(0)\rangle = |\psi(0)\rangle$ is the probe's ferromagnetic initial state, and τ_i is the evolution time between the $i-1$ and i measurements. After gathering a trajectory of length n_{seq} of outcomes $\boldsymbol{\gamma} = (\gamma_1, \gamma_2, \ldots, \gamma_{n_{\text{seq}}})$, the probe is reset and the process is repeated to generate a new trajectory. The protocol does not need any prior entanglement, as it is built up naturally during the evolution. Because of the entanglement between the readout qubit and the rest of the system, the quantum state of the system after the wave function collapses still carries information about the local field, which further helps the sensing in the next sequence. Note that the conventional sensing is a special case of our sequential protocol with $n_{\text{seq}} = 1$.

Classical precision bound.—The sensing precision for estimating $\boldsymbol{B} = (B_x, 0, 0)$ given a measurement basis (here σ_N^z) is determined by the classical Fisher information

$$\mathcal{F}(B_x) = \sum_{\boldsymbol{\gamma}}\frac{1}{P_{\boldsymbol{\gamma}}}\left(\frac{\partial P_{\boldsymbol{\gamma}}}{\partial B_x}\right)^2, \qquad P_{\boldsymbol{\gamma}} = \prod_{i=1}^{n_{\text{seq}}} p_{\gamma_i}^{(i)}. \tag{2}$$

In the above, $P_{\boldsymbol{\gamma}}$ is the probability of obtaining the trajectory $\boldsymbol{\gamma}$ and the $\sum_{\boldsymbol{\gamma}}$ runs over $2^{n_{\text{seq}}}$ configurations from $\boldsymbol{\gamma} = (\downarrow, \downarrow, \ldots, \downarrow)$ to $\boldsymbol{\gamma} = (\uparrow, \uparrow, \ldots, \uparrow)$. To see the impact of sequential measurements on the precision of sensing, in Fig. 2(a) we plot the inverse of classical Fisher information $\mathcal{F}^{-1}$, as the bound in the Cramér-Rao inequality, versus n_{seq} for two different probe lengths N when the unknown parameter B_x is set to be $B_x = 0.1J$ and $\tau_i = \tau = 5/J$ for all sequences. As the figure clearly shows, $\mathcal{F}^{-1}$ decreases very rapidly by increasing n_{seq}, indicating the significant advantage of sequential measurements for enhancing the sensing precision. Our numerical data can be fit by $g(n_{\text{seq}}) = \alpha n_{\text{seq}}^{-\beta} + \epsilon$, in which ϵ is vanishingly small and β is always found to be $\beta > 1$. This is indeed an

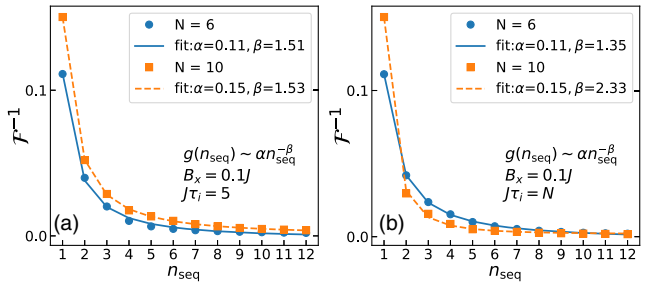

FIG. 2. Inverse of the Fisher information $\mathcal{F}^{-1}$ as a function of the number of sequential measurements n_{seq} performed at site N for $B_x = 0.1J$. We consider two cases for the time interval between measurements: (a) $J\tau_i = 5$ and (b) $J\tau_i = N$. A fitting function $g(n_{\text{seq}})$ with exponent $\beta > 1$ is shown.

indicator of possible quantum-enhanced sensitivity beyond the standard limit, which will be discussed later. Note that, for larger system sizes, the probe needs more time to transfer information from site 1 to site N, and thus, τ has to be larger. Our numerical investigations show that $\tau \sim N/J$ provides the best estimation. To evidence this, in Fig. 2(b) we plot $\mathcal{F}^{-1}$ as a function of n_{seq} when $\tau_i = \tau = N/J$ for all sequences. In contrast to Fig. 2(a), the performance of the longer probe becomes better for this choice of τ. This is an interesting observation, as it shows that using a longer probe facilitates remote sensing and achieves better precision.

Bayesian estimation.—While Fisher information provides a bound for precision, one always needs to use an estimator to actually infer the value of the unknown parameter. Here, we feed the experimental data into a Bayesian estimator, which is known to be optimal for achieving the Cramér-Rao bound [32,88–98]. By repeating the procedure for M times, one gets a set of $\mathbf{\Gamma} = \{\boldsymbol{\gamma}_1, \boldsymbol{\gamma}_2, \ldots, \boldsymbol{\gamma}_M\}$, where each trajectory $\boldsymbol{\gamma}_k$ contains n_{seq} spin outcomes. Therefore, the total number of measurements performed on the probe is $n_{\mathrm{seq}}M$. By assuming a uniform prior over the interval of interest, which is assumed to be $B_x \in [-0.2J, 0.2J]$, one can estimate the posterior distribution $f(B_x|\mathbf{\Gamma})$. For detailed discussions, see the Supplemental Material [87]. There are numerous ways to infer $\widehat{B_x}$ as the estimate for B_x. Here, we assume that $\widehat{B_x}$ is directly sampled from the posterior distribution $f(B_x|\mathbf{\Gamma})$. Since $\widehat{B_x}$ is sampled from the probability distribution $f(B_x|\mathbf{\Gamma})$, one can quantify the quality of the estimation by defining the dimensionless average squared relative error as

$$\delta B_x^2 = \int f(\hat{B}_x|\mathbf{\Gamma}) \left(\frac{|\hat{B}_x - B_x|}{|B_x|} \right)^2 d\hat{B}_x, \tag{3}$$

where the integration is over the interval of interest, and $|\hat{B}_x - B_x|/|B_x|$ is the relative error of the estimation. A direct calculation simplifies the above figure of merit as

$$\delta B_x^2 = \frac{\sigma^2 + |\langle B_x \rangle - B_x|^2}{|B_x|^2}, \tag{4}$$

where σ^2 and $\langle B_x \rangle$ are the variance and the average of the magnetic field with respect to the posterior distribution, respectively. The average squared relative error simultaneously quantifies the uncertainty of estimation (i.e., σ) as well as the bias in the estimation (i.e., $\langle B_x \rangle - B_x$). In the case of an unbiased estimator, δB_x is reduced to $\sigma/|B_x|$, which is the inverse of the signal-to-noise ratio.

In Fig. 3(a), we plot the posterior as a function of B_x/J when the actual value is $B_x = 0.1J$ for different values of n_{seq}. By increasing the number of sequences, the posterior gets narrower, indicating enhancement of the precision. To show the generality of this across all values of B_x, one can compute the average of δB_x^2 for 100 different samples, denoted by $\overline{\delta B_x^2}$, at each value of B_x/J. In Fig. 3(b), we plot $\overline{\delta B_x^2}$ as a function of B_x/J for a probe of length $N = 6$ and two different values of n_{seq}. Evidenced by the figure, increasing n_{seq} significantly enhances the precision across the whole range of B_x/J. Note that, as B_x/J tends to zero, the average error diverges due to the presence of B_x in the denominator of Eq. (3).

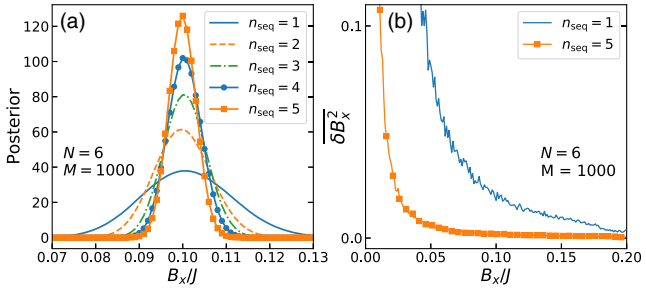

FIG. 3. (a) Posterior distribution as a function of B_x/J for several n_{seq} for sensing $B_x = 0.1J$. (b) Average of δB_x^2 as a function of B_x/J for two values of n_{seq}, where each point is averaged over 100 samples. In both panels, the posterior is obtained by repeating the procedure for $M = 1000$ times in a probe of $N = 6$ with fixed $J\tau_i = N$.

Trajectory-based sensing.—Recently, a numerical analysis [99], which was followed by analytical proof [100], has shown that by using a single long trajectory $\boldsymbol{\gamma}$ with $n_{\mathrm{seq}} \gg 1$ one can reduce the variance of the posterior distribution such that one can asymptotically reach $f(B_x|\boldsymbol{\gamma}) = \delta(B_x - B_x^{\mathrm{real}})$, where B_x^{real} is the real value of B_x and $\delta(x)$ is the Dirac delta function. This means that a single trajectory with $n_{\mathrm{seq}} \gg 1$ is indeed enough to provide an estimation of arbitrary precision. However, it is unclear how the precision scales with n_{seq}. In what follows, we numerically address this issue.

Time as resource.—From a practical point of view, the total time spent for accomplishing the sensing is the main resource to determine the performance of a sensing protocol. While the coherent time evolution of a quantum system is fast, measurement and initialization empirically are 1 and 2 orders of magnitude slower, respectively [10]. Therefore, for a given total time, it would be highly beneficial to reduce the number of initialization and use the saved time for increasing the number of measurements. This time compensation allows for a better inference of the information content about the quantity of interest. The total time can be written as

$$T = M(t_{\mathrm{init}} + t_{\mathrm{evo}} + t_{\mathrm{meas}} n_{\mathrm{seq}}), \tag{5}$$

where t_{init}, t_{evo}, and t_{meas} are the initialization, evolution, and measurement times, respectively. By fixing $\tau_i = \tau = N/J$, one gets $t_{\mathrm{evo}} = n_{\mathrm{seq}}\tau$. In addition, we fixed $t_{\mathrm{init}} = 600/J$ and $t_{\mathrm{meas}} = 50/J$, to be consistent with experimental

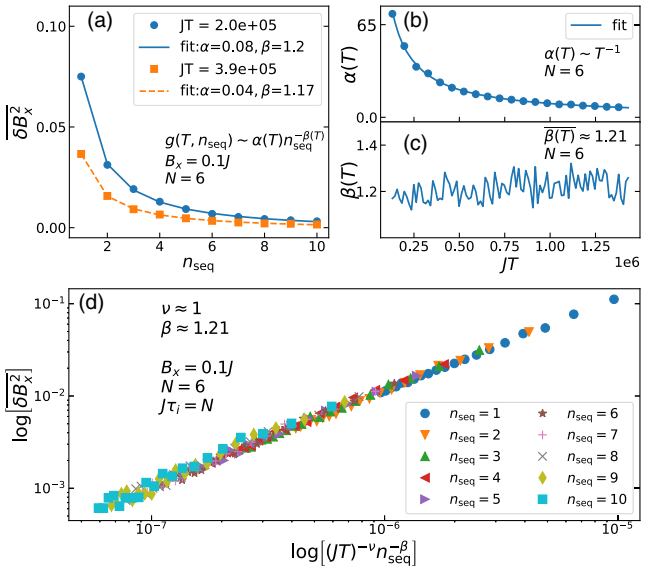

FIG. 4. Estimating $B_x = 0.1J$ with a probe of $N = 6$ and $J\tau_i = N$. (a) Averaged squared relative error $\overline{\delta B_x^2}$ versus n_{seq} for two total execution times T. (b) Fitting coefficient $\alpha(T)$ as function of time T. (c) Fitting exponent $\beta(T)$ as function of time. (d) Universal behavior of $\overline{\delta B_x^2}$ versus $(JT)^{-\nu} n_{\mathrm{seq}}^{-\beta}$ for several values of n_{seq} and total time T.

values [10]. For a given total time T, the choice of n_{seq} changes the reinitialization M and thus the total number of measurements. In Fig. 4(a), we plot $\overline{\delta B_x^2}$ computed through Bayesian estimation for $B_x = 0.1J$, as a function of n_{seq} for two given values of T. Up to a vanishingly small constant, one can use the fitting function $g(T, n_{\mathrm{seq}}) = \alpha(T) n_{\mathrm{seq}}^{-\beta(T)}$. To have a proper resource analysis, one has to determine the dependence of $\alpha(T)$ and $\beta(T)$ exponents with respect to total time T. In Figs. 4(b) and 4(c), we plot $\alpha(T)$ and $\beta(T)$ as a function of time. While $\alpha(T)$ shows clear dependence on time as $\alpha(T) \sim T^{-\nu}$, with $\nu \to 1$, the exponent $\beta(T)$ fluctuates around 1.21. Thus, the fitting function is reduced to

$$\overline{\delta B_x^2} \sim T^{-\nu} n_{\mathrm{seq}}^{-\beta}. \tag{6}$$

This is the main result of our Letter. Note that, although $\nu \sim 1$, one should not be misled by interpreting it as standard scaling. The key point is that, for a fixed total time T, one can always enhance the precision by increasing n_{seq}. In Fig. 4(d), we show the universal behavior of Eq. (6), through choosing different values of T and n_{seq}. To better understand the dependence of $\overline{\delta B_x^2}$ on time T, one can get $n_{\mathrm{seq}} = (T - M t_{\mathrm{init}})/M(\tau + t_{\mathrm{meas}})$ from Eq. (5) and replace it in Eq. (6). For $T \gg M t_{\mathrm{init}}$, one obtains

$$\overline{\delta B_x^2} \sim T^{-(\nu+\beta)}. \tag{7}$$

As $\nu \sim 1$ and $\beta > 1$, one can see that quantum-enhanced sensing can indeed be achieved. Note that the condition $T \gg M t_{\mathrm{init}}$ can always be satisfied by decreasing the reinitialization M and spending all the time resource T on sequential measurements. In the extreme case of $M = 1$ ($n_{\mathrm{seq}} \gg 1$), one could truly achieve the scaling of Eq. (7). It is also worth emphasizing that, though $\beta > 1$ suggests that our protocol can asymptotically achieve super-Heisenberg scaling (namely, $\beta + \nu > 2$), one has to be careful for this generalization in the limit of $n_{\mathrm{seq}} \gg 1$. Therefore, a more careful investigation remains open for verifying a possible super-Heisenberg precision.

Protocol robustness.—We consider two sources of imperfections, namely, dephasing and disordered couplings. As we quantitatively show in the Supplemental Material [87], both of these imperfections are destructive for sensing. Nonetheless, quantum-enhanced sensitivity, i.e., superlinear scaling of $\mathcal{F}$, can be found until dephasing or disorder strength are greater than a threshold value. Beyond these threshold values, $\mathcal{F}$ scales linearly with n_{seq} and quantum-enhanced sensitivity is lost. Our numerical simulations, see Supplemental Material [87], show that for both dephasing and disorder strengths of up to $\sim 5\% J$ the quantum-enhanced sensitivity can be achieved.

Two-parameter estimation.—For the sake of completeness, we also consider two-parameter sensing, in which both B_x and B_z are nonzero. In this case, a single σ_N^z measurement is not enough to estimate both of the parameters. Hence, we consider a positive operator-valued measure built from the eigenvectors of σ_N^z and σ_N^x [87]. To exemplify the performance of our protocol, we consider $\boldsymbol{B} = (0.15, 0, 0.1)J$, and for a given time T we perform Bayesian analysis for two values of n_{seq}. In Figs. 5(a) and 5(b), we plot the posterior $f(\boldsymbol{B}|\boldsymbol{\Gamma})$ in the plane of B_x/J and B_z/J for $n_{\mathrm{seq}} = 1$ and $n_{\mathrm{seq}} = 7$, respectively. Remarkably, the posterior shrinks significantly as n_{seq} increases, indicating the effectiveness of sequential measurements for enhancing the precision for a given time. To further clarify this, we can generalize the average squared relative error in Eq. (3) by replacing B_x with $\boldsymbol{B}$ (and $|\cdot|$ represents the norm of the vector) to obtain $\overline{\delta \boldsymbol{B}^2}$. In Fig. 5(c), we plot $\overline{\delta \boldsymbol{B}^2}$ as a function of n_{seq} for $\boldsymbol{B} = (0.15, 0, 0.1)J$, which shows rapid

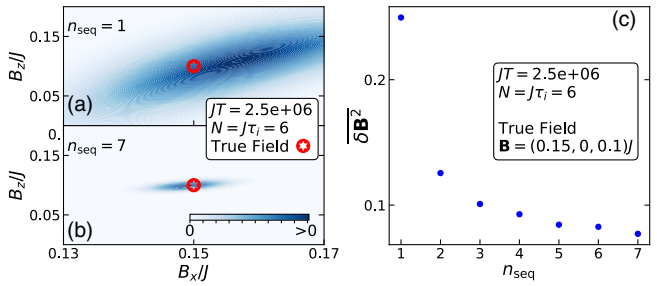

FIG. 5. (a) and (b) Posterior distributions for $n_{\mathrm{seq}} = 1$ and $n_{\mathrm{seq}} = 7$ for the estimation of $\boldsymbol{B} = (0.15, 0, 0.1)J$, respectively. (c) Averaged squared relative error $\overline{\delta \boldsymbol{B}^2}$ as a function of n_{seq}.

enhancement as the number of sequences increases. This clearly shows the generality of our protocol for multiparameter sensing.

Conclusions.—We propose a protocol for remotely sensing a local magnetic field through a sequence of local measurements performed on a single qubit of a quantum many-body probe initialized in a product state. By increasing the sequence of measurements, one can avoid the time-consuming probe's reinitialization, allowing for taking more measurements within the same amount of time. This naturally enhances the sensing precision, which asymptotically reaches the Heisenberg bound. Unlike previous schemes, our procedure utilizes the nature of quantum measurement and its subsequent wave function collapse and thus avoids the need for complex initial entangled states, quantum criticality, and adaptive measurements. Unlike the protocols based on deferred measurement schemes [101], our protocol neither requires ancilla qubits nor relies on feedback control. Thus, our minimal control scheme is expected to be less demanding for practical implementations.

A. B. acknowledges support from the National Key R&D Program of China (Grant No. 2018YFA0306703), the National Science Foundation of China (Grants No. 12050410253 and No. 92065115), and the Ministry of Science and Technology of China (Grant No. QNJ2021167001L). V. M. thanks the National Natural Science Foundation of China (Grant No. 12050410251), the Chinese Postdoctoral Science Fund (Grant No. 2018M643435), and the Ministry of Science and Technology of China (Grant No. QNJ2021167004). S. B. acknowledges the EPSRC grant for nonergodic quantum manipulation (Grant No. EP/R029075/1).

*Corresponding author.
vmontenegro@uestc.edu.cn
†gareth.jones.16@ucl.ac.uk
‡s.bose@ucl.ac.uk
§Corresponding author.
abolfazl.bayat@uestc.edu.cn

[1] C. L. Degen, F. Reinhard, and P. Cappellaro, Rev. Mod. Phys. **89**, 035002 (2017).
[2] D. Braun, G. Adesso, F. Benatti, R. Floreanini, U. Marzolino, M. W. Mitchell, and S. Pirandola, Rev. Mod. Phys. **90**, 035006 (2018).
[3] S. Pirandola, B. R. Bardhan, T. Gehring, C. Weedbrook, and S. Lloyd, Nat. Photonics **12**, 724 (2018).
[4] M. W. Mitchell, J. S. Lundeen, and A. M. Steinberg, Nature (London) **429**, 161 (2004).
[5] T. Nagata, R. Okamoto, J. L. O'Brien, K. Sasaki, and S. Takeuchi, Science **316**, 726 (2007).
[6] M. A. Taylor, J. Janousek, V. Daria, J. Knittel, B. Hage, H.-A. Bachor, and W. P. Bowen, Nat. Photonics **7**, 229 (2013).
[7] Z. Hou, R.-J. Wang, J.-F. Tang, H. Yuan, G.-Y. Xiang, C.-F. Li, and G.-C. Guo, Phys. Rev. Lett. **123**, 040501 (2019).
[8] R. Liu, Y. Chen, M. Jiang, X. Yang, Z. Wu, Y. Li, H. Yuan, X. Peng, and J. Du, npj Quantum Inf. **7**, 170 (2021).
[9] J. Taylor, P. Cappellaro, L. Childress, L. Jiang, D. Budker, P. Hemmer, A. Yacoby, R. Walsworth, and M. Lukin, Nat. Phys. **4**, 810 (2008).
[10] C. Bonato, M. Blok, H. Dinani, D. Berry, M. Markham, D. Twitchen, and R. Hanson, Nat. Nanotechnol. **11**, 247 (2016).
[11] M. Blok, C. Bonato, M. Markham, D. Twitchen, V. Dobrovitski, and R. Hanson, Nat. Phys. **10**, 189 (2014).
[12] D. Leibfried, M. D. Barrett, T. Schaetz, J. Britton, J. Chiaverini, W. M. Itano, J. D. Jost, C. Langer, and D. J. Wineland, Science **304**, 1476 (2004).
[13] M. J. Biercuk, H. Uys, A. P. VanDevender, N. Shiga, W. M. Itano, and J. J. Bollinger, Nature (London) **458**, 996 (2009).
[14] R. Maiwald, D. Leibfried, J. Britton, J. C. Bergquist, G. Leuchs, and D. J. Wineland, Nat. Phys. **5**, 551 (2009).
[15] I. Baumgart, J.-M. Cai, A. Retzker, M. B. Plenio, and C. Wunderlich, Phys. Rev. Lett. **116**, 240801 (2016).
[16] J. G. Bohnet, B. C. Sawyer, J. W. Britton, M. L. Wall, A. M. Rey, M. Foss-Feig, and J. J. Bollinger, Science **352**, 1297 (2016).
[17] J. Bylander, S. Gustavsson, F. Yan, F. Yoshihara, K. Harrabi, G. Fitch, D. G. Cory, Y. Nakamura, J.-S. Tsai, and W. D. Oliver, Nat. Phys. **7**, 565 (2011).
[18] M. Bal, C. Deng, J.-L. Orgiazzi, F. Ong, and A. Lupascu, Nat. Commun. **3**, 1324 (2012).
[19] F. Yan, S. Gustavsson, J. Bylander, X. Jin, F. Yoshihara, D. G. Cory, Y. Nakamura, T. P. Orlando, and W. D. Oliver, Nat. Commun. **4**, 2337 (2013).
[20] W. Wang, Y. Wu, Y. Ma, W. Cai, L. Hu, X. Mu, Y. Xu, Z.-J. Chen, H. Wang, Y. Song *et al.*, Nat. Commun. **10**, 1 (2019).
[21] V. Montenegro, M. G. Genoni, A. Bayat, and M. G. A. Paris, Phys. Rev. Research **4**, 033036 (2022).
[22] V. Montenegro, M. G. Genoni, A. Bayat, and M. G. A. Paris, Phys. Rev. Research **2**, 043338 (2020).
[23] T. Bagci, A. Simonsen, S. Schmid, L. G. Villanueva, E. Zeuthen, J. Appel, J. M. Taylor, A. Sørensen, K. Usami, A. Schliesser *et al.*, Nature (London) **507**, 81 (2014).
[24] S. Qvarfort, A. Serafini, P. F. Barker, and S. Bose, Nat. Commun. **9**, 3690 (2018).
[25] S. Qvarfort, A. D. K. Plato, D. E. Bruschi, F. Schneiter, D. Braun, A. Serafini, and D. Rätzel, Phys. Rev. Research **3**, 013159 (2021).
[26] J. Appel, P. J. Windpassinger, D. Oblak, U. B. Hoff, N. Kjærgaard, and E. S. Polzik, Proc. Natl. Acad. Sci. U.S.A. **106**, 10960 (2009).
[27] I. D. Leroux, M. H. Schleier-Smith, and V. Vuletić, Phys. Rev. Lett. **104**, 073602 (2010).
[28] A. Louchet-Chauvet, J. Appel, J. J. Renema, D. Oblak, N. Kjaergaard, and E. S. Polzik, New. J. Phys. **12**, 065032 (2010).
[29] R. J. Sewell, M. Koschorreck, M. Napolitano, B. Dubost, N. Behbood, and M. W. Mitchell, Phys. Rev. Lett. **109**, 253605 (2012).
[30] J. G. Bohnet, K. C. Cox, M. A. Norcia, J. M. Weiner, Z. Chen, and J. K. Thompson, Nat. Photonics **8**, 731 (2014).

[31] O. Hosten, N. J. Engelsen, R. Krishnakumar, and M. A. Kasevich, Nature (London) **529**, 505 (2016).
[32] M. Paris, Int. J. Quantum. Inform. **07**, 125 (2009).
[33] J. Liu, H. Yuan, X.-M. Lu, and X. Wang, J. Phys. A **53**, 023001 (2020).
[34] P. Cappellaro, Phys. Rev. A **85**, 030301(R) (2012).
[35] N. Nusran, M. Momeen, and M. Dutt, Nat. Nanotechnol. **7**, 109 (2012).
[36] G. Waldherr, J. Beck, P. Neumann, R. Said, M. N, M. M, D. Twitchen, J. Twamley, F. Jelezko, and J. Wrachtrup, Nat. Nanotechnol. **7**, 105 (2012).
[37] R. S. Said, D. W. Berry, and J. Twamley, Phys. Rev. B **83**, 125410 (2011).
[38] V. Giovannetti, S. Lloyd, and L. Maccone, Science **306**, 1330 (2004).
[39] V. Giovannetti, S. Lloyd, and L. Maccone, Phys. Rev. Lett. **96**, 010401 (2006).
[40] V. Giovannetti, S. Lloyd, and L. Maccone, Nat. Photonics **5**, 222 (2011).
[41] L. Garbe, O. Abah, S. Felicetti, and R. Puebla, arXiv: 2112.11264v2.
[42] F. Fröwis and W. Dür, Phys. Rev. Lett. **106**, 110402 (2011).
[43] R. Demkowicz-Dobrzański, J. Kołodyński, and M. Guţă, Nat. Commun. **3**, 1063 (2012).
[44] K. Wang, X. Wang, X. Zhan, Z. Bian, J. Li, B. C. Sanders, and P. Xue, Phys. Rev. A **97**, 042112 (2018).
[45] H. Kwon, K. C. Tan, T. Volkoff, and H. Jeong, Phys. Rev. Lett. **122**, 040503 (2019).
[46] D. M. Greenberger, M. A. Horne, and A. Zeilinger, in *Bell's Theorem, Quantum Theory and Conceptions of the Universe* (Springer, New York, 1989), pp. 69–72.
[47] P. Zanardi and N. Paunković, Phys. Rev. E **74**, 031123 (2006).
[48] P. Zanardi, H. T. Quan, X. Wang, and C. P. Sun, Phys. Rev. A **75**, 032109 (2007).
[49] P. Zanardi, M. G. A. Paris, and L. Campos Venuti, Phys. Rev. A **78**, 042105 (2008).
[50] C. Invernizzi, M. Korbman, L. C. Venuti, and M. G. A. Paris, Phys. Rev. A **78**, 042106 (2008).
[51] S.-J. Gu, Int. J. Mod. Phys. B **24**, 4371 (2010).
[52] M. Skotiniotis, P. Sekatski, and W. Dür, New. J. Phys. **17**, 073032 (2015).
[53] Y. Chu, S. Zhang, B. Yu, and J. Cai, Phys. Rev. Lett. **126**, 010502 (2021).
[54] V. Montenegro, U. Mishra, and A. Bayat, Phys. Rev. Lett. **126**, 200501 (2021).
[55] S. Sarkar, C. Mukhopadhyay, A. Alase, and A. Bayat, Phys. Rev. Lett. **129**, 090503 (2022).
[56] M. M. Rams, P. Sierant, O. Dutta, P. Horodecki, and J. Zakrzewski, Phys. Rev. X **8**, 021022 (2018).
[57] L. Garbe, M. Bina, A. Keller, M. G. A. Paris, and S. Felicetti, Phys. Rev. Lett. **124**, 120504 (2020).
[58] U. Mishra and A. Bayat, Phys. Rev. Lett. **127**, 080504 (2021).
[59] U. Mishra and A. Bayat, arXiv:2105.13507.
[60] B. L. Higgins, D. W. Berry, S. D. Bartlett, H. M. Wiseman, and G. J. Pryde, Nature (London) **450**, 393 (2007).
[61] D. W. Berry, B. L. Higgins, S. D. Bartlett, M. W. Mitchell, G. J. Pryde, and H. M. Wiseman, Phys. Rev. A **80**, 052114 (2009).
[62] B. Higgins, D. Berry, S. Bartlett, M. Mitchell, H. Wiseman, and G. Pryde, New J. Phys. **11**, 073023 (2009).
[63] S. Gammelmark and K. Mølmer, Phys. Rev. Lett. **112**, 170401 (2014).
[64] M. A. C. Rossi, F. Albarelli, D. Tamascelli, and M. G. Genoni, Phys. Rev. Lett. **125**, 200505 (2020).
[65] F. Albarelli, M. A. C. Rossi, M. G. A. Paris, and M. G. Genoni, New J. Phys. **19**, 123011 (2017).
[66] J. J. Meyer, J. Borregaard, and J. Eisert, npj-Quantum Inf. **7**, 1 (2021).
[67] C. D. Marciniak, T. Feldker, I. Pogorelov, R. Kaubruegger, D. V. Vasilyev, R. van Bijnen, P. Schindler, P. Zoller, R. Blatt, and T. Monz, Nature (London) **603**, 604 (2022).
[68] J. Yang, S. Pang, Z. Chen, A. N. Jordan, and A. del Campo, Phys. Rev. Lett. **128**, 160505 (2022).
[69] J. Kołodyński and R. Demkowicz-Dobrzański, New J. Phys. **15**, 073043 (2013).
[70] R. Demkowicz-Dobrzański, J. Kołodyński, and M. Guţă, Nat. Commun. **3**, 1063 (2012).
[71] F. Albarelli, M. A. C. Rossi, D. Tamascelli, and M. G. Genoni, Quantum **2**, 110 (2018).
[72] S. Boixo, S. T. Flammia, C. M. Caves, and J. M. Geremia, Phys. Rev. Lett. **98**, 090401 (2007).
[73] A. De Pasquale, D. Rossini, P. Facchi, and V. Giovannetti, Phys. Rev. A **88**, 052117 (2013).
[74] S. Pang and T. A. Brun, Phys. Rev. A **90**, 022117 (2014).
[75] J. R. McClean, S. Boixo, V. N. Smelyanskiy, R. Babbush, and H. Neven, Nat. Commun. **9**, 4812 (2018).
[76] A. Bayat, Phys. Rev. Lett. **118**, 036102 (2017).
[77] D. K. Burgarth, P. Facchi, V. Giovannetti, H. Nakazato, S. Pascazio, and K. Yuasa, Nat. Commun. **5**, 5173 (2014).
[78] S. Pouyandeh, F. Shahbazi, and A. Bayat, Phys. Rev. A **90**, 012337 (2014).
[79] W.-L. Ma, P. Wang, W.-H. Leong, and R.-B. Liu, Phys. Rev. A **98**, 012117 (2018).
[80] A. Bayat, B. Alkurtass, P. Sodano, H. Johannesson, and S. Bose, Phys. Rev. Lett. **121**, 030601 (2018).
[81] S. Choi, Y. Bao, X.-L. Qi, and E. Altman, Phys. Rev. Lett. **125**, 030505 (2020).
[82] S.-K. Jian, C. Liu, X. Chen, B. Swingle, and P. Zhang, Phys. Rev. Lett. **127**, 140601 (2021).
[83] T. Minato, K. Sugimoto, T. Kuwahara, and K. Saito, Phys. Rev. Lett. **128**, 010603 (2022).
[84] B. Skinner, J. Ruhman, and A. Nahum, Phys. Rev. X **9**, 031009 (2019).
[85] M. J. Gullans and D. A. Huse, Phys. Rev. X **10**, 041020 (2020).
[86] M. Block, Y. Bao, S. Choi, E. Altman, and N. Y. Yao, Phys. Rev. Lett. **128**, 010604 (2022).
[87] See Supplemental Material at http://link.aps.org/supplemental/10.1103/PhysRevLett.129.120503 clarifies aspects of the remote feature of our sensing protocol, some brief elements on Bayesian estimation, the general case for the estimation of a multicomponent local magnetic field, and the robustness of our protocol in the presence of noise and decoherence.
[88] H. Cramér, *Mathematical Methods of Statistics* (Princeton University Press, Princeton, NJ, 1999), Vol. 43.
[89] C. Helstrom, Phys. Lett. **25A**, 101 (1967).

[90] A. Holevo, in *Quantum Probability and Applications to the Quantum Theory of Irreversible Processes* (Springer, New York, 1984), pp. 153–172.
[91] S. L. Braunstein and C. M. Caves, Phys. Rev. Lett. **72**, 3439 (1994).
[92] S. Braunstein, Phys. Lett. A **219**, 169 (1996).
[93] G. Goldstein, M. Lukin, and P. Capellaro, arXiv:1001.4804.
[94] L. M. Le Cam, *Asymptotic Methods in Statistical Decision Theory*, Springer Series in Statistics (Springer-Verlag, New York, 1986).
[95] Z. Hradil, R. Myška, J. Peřina, M. Zawisky, Y. Hasegawa, and H. Rauch, Phys. Rev. Lett. **76**, 4295 (1996).
[96] L. Pezzé, A. Smerzi, G. Khoury, J. F. Hodelin, and D. Bouwmeester, Phys. Rev. Lett. **99**, 223602 (2007).
[97] J. Rubio and J. Dunningham, New J. Phys. **21**, 043037 (2019).
[98] S. Olivares and M. G. A. Paris, J. Phys. B **42**, 055506 (2009).
[99] P. Six, Ph. Campagne-Ibarcq, L. Bretheau, B. Huard, and P. Rouchon, in *Proceedings of the 54th IEEE Annual Conference on Decision and Control (CDC)* (IEEE, Osaka, 2015), pp. 7742–7748.
[100] M. Bompais, N. H. Amini, and C. Pellegrini, arXiv:2204.00343.
[101] S. Boixo, S. T. Flammia, C. M. Caves, and J. M. Geremia, Phys. Rev. Lett. **98**, 090401 (2007).